Electron-cadmium ionization for energies near overlapping autoionizing resonances

M. M. Tabanli, J. L. Peacher, and D. H. Madison
Department of Physics, University of Missouri–Rolla, Rolla, Missouri 65409-0640
(Received 14 September 2001; published 2 April 2002)

The effect of autoionizing resonances on ionization has been studied since the historic work of Fano. In the autoionization problem, it is not possible to distinguish electrons, that have been directly ejected from the atom, from those that were first excited to an autoionizing resonance level because of the extremely short lifetime. As a result, these two processes will interfere. Furthermore if the energy difference between the resonances is not larger than the width of the resonances, the resonances will also interfere with each other. In this paper, we examine electron-impact ionization $(e,2e)$ for cadmium in the energy range where the autoionizing resonances overlap and interfere. First-order distorted-wave results will be compared with recent measurements and previous calculations.

DOI: 10.1103/PhysRevA.65.042718 PACS number(s): 34.80.Dp, 32.80.Dz

I. INTRODUCTION

The theory of photoionization with autoionizing resonances is well understood and has been studied following the theoretical analysis as developed by Fano and co-workers [1,2]. In Fano's approach the Hamiltonian was diagonalized using the interaction of the discrete excited states with the continuum via the Coulomb interaction. He stated his result for the transition amplitude (T matrix) by defining the well-known q parameter. Shore [3] obtained an alternative parametrization for the differential cross section. The relation between the Shore and Fano parameters have been shown by McDonald and Crowe [4]. Later Davis and Feldkamp [5] generalized Fano's theoretical results to the case of multiple-overlapping-autoionization resonances and gave an easy-to-use formula for calculating the transition amplitude. Balashov *et al.* [6,7] have generalized Fano's results for photoionization to the case of electron-impact ionization, in which the ejected-electron angle dependence of the differential cross section is first introduced. Their results reduce to Fano's results when integrated over the ejected-electron angles. There are a number of calculations of the Fano and/or Shore parameters or directly the differential cross section for the $(e,2e)$ process. Most of the work has concentrated on helium. The theoretical work of Balashov *et al.* [6,7], Kheifets [8], measurements and calculations of Pochat *et al.* [9], McDonald and Crowe [10], Samardzic *et al.* [11,12] have all concentrated on helium. In the situation where there are multiple resonances, they are treated as nonoverlapping. Although some work on autoionization has been done on $(e,2e)$ for heavier atoms, experiment on argon by Stefani *et al.* [13], experiment on neon by Zhong *et al.* [14], experiment on Al^{2+} ion by Thomason and Peart [15], calculation on Al^{2+} ion by Teng [16], experiment on krypton by Khouilid *et al.* [17], there are still very few studies on overlapping resonances. There have been many studies on autoionization in photoionization as well. However we have confined ourselves to the electron-impact ionization process in this paper.

Our approach is to generalize the theoretical treatment of Balashov *et al.* [6,7] for helium to heavier atoms with an emphasis on overlapping resonances. For the triple differential cross section we have used the basic formulas for photoexcitation given by Davis and Feldkamp [5] [Eqs. (53) and (54)] and modified them for electron ionization by adding the ejected-electron angular dependence using the technique described by Balashov *et al.* [6,7]. We have applied our results to e-Cd scattering. This study was motivated by experiments performed by Martin and co-workers [18–21]. Both Madison *et al.* [22] and Martin *et al.* [20,21] have done calculations for triple differential cross sections (TDCSs) on the e-Cd autoionization problem using a ''nonoverlapping-resonances'' approach. Both have fairly good agreement with experiment only for scattering angles less than 7°.

II. THEORY

This paper introduces a model to calculate the T matrix for $(e,2e)$ processes for which the energy of one of the final-state continuum electrons is near an autoionizing level. In this case, it is not possible to determine if an observed electron comes from direct ionization or from autoionization. Thus this process is a coherent sum of two different amplitudes,

$$|T_{total}(\mathbf{k}_0,\mathbf{k}_a,\mathbf{k}_b)|^2=\frac{1}{2}\sum_{\mu_i,\mu_b,\mu_0,\mu_a}|(T_{dir})^{\mu_i,\mu_b}_{\mu_0,\mu_a}(\mathbf{k}_0,\mathbf{k}_a,\mathbf{k}_b)+(T_{res})^{\mu_i,\mu_b}_{\mu_0,\mu_a}(\mathbf{k}_0,\mathbf{k}_a,\mathbf{k}_b)|^2. \quad (1)$$

Here $\mathbf{k}_0$, $\mathbf{k}_a$, and $\mathbf{k}_b$ are the momenta vectors for the initial, scattered, and ejected electrons. The quantities μ_0, μ_a, and μ_b are the spin projections for the incident, scattered, and ejected electrons, respectively; and μ_i is the total spin projection of the residual ion. The theory should also include a sum over all other possible final states of the ion. However for the system studied here there is only one possible final state. Since both ejected and scattered electrons are indistinguishable, instead of labeling them as scattered and ejected electrons it is more convenient to label them as fast and slow electrons. The $(T_{dir})^{\mu_i,\mu_b}_{\mu_0,\mu_a}(\mathbf{k}_0,\mathbf{k}_a,\mathbf{k}_b)$ term is the direct-

ionization amplitude and the $(T_{res})^{\mu_i,\mu_b}_{\mu_0,\mu_a}(\mathbf{k}_0,\mathbf{k}_a,\mathbf{k}_b)$ term is the resonance (-autoionization) amplitude. The following sections will discuss how we calculate $(T_{res})^{\mu_i,\mu_b}_{\mu_0,\mu_a}(\mathbf{k}_0,\mathbf{k}_a,\mathbf{k}_b)$.

A. Nonoverlapping resonances treatment

Fano derived a formula for the resonance amplitude for photoionization. For a single resonance, Balashov *et al.* [6,7] showed that for the $(e,2e)$ process the resonance part of the T matrix can be written as

$$(T^r_{res})^{\mu_i,\mu_b}_{\mu_0,\mu_a}(\mathbf{k}_0,\mathbf{k}_a,\mathbf{k}_b)=C(E_b)[(T^r_{dis})^{\mu_i,\mu_b}_{\mu_0,\mu_a}(\mathbf{k}_0,\mathbf{k}_a,\mathbf{k}_b) - i\pi V_r^*(T^r_{con})^{\mu_i,\mu_b}_{\mu_0,\mu_a}(\mathbf{k}_0,\mathbf{k}_a,\mathbf{k}_b)], \tag{2}$$

where r labels the particular resonance. We label $r=1,2,3,\ldots$, where $r=1$ corresponds to the lowest energy resonance and so on. The energy of the autoionizing resonance is E_r and the energy of the ejected electron is E_b. Here T^r_{dis} is the excitation amplitude coming from the discrete part of the total wave function and T^r_{con} is the ionization amplitude coming from the continuum part of the total wave function in the Fano sense. They are both calculated at a specific resonance energy E_r. Once the energies of the incident and ejected electrons are given, conservation of energy dictates the energy of the scattered electron. Therefore T^r_{dis} and T^r_{con} do not depend explicitly on the energy of the scattered electron. Fano's factor $C(E_b)$ contains the only explicit ejected-electron energy dependence of T^r_{res}. It is given by

$$C(E_b)=\frac{1}{(\epsilon_r+i)\pi V_r^*}. \tag{3}$$

The parameter ϵ_r is defined to be the energy deviation from the resonant energy in units of the resonance half-width. Thus

$$\epsilon_r=\frac{E_b-E_r}{\Gamma_r/2}, \tag{4}$$

where Γ_r is the full width at half maximum for the resonance. The interaction strength V_r is defined as

$$V_r=\langle\psi(E_r)|V_{1,2}|\Phi_r\rangle, \tag{5}$$

where $V_{1,2}$ is the Coulomb interaction between the two electrons, one of which will autoionize. The ket $|\Phi_r\rangle$ is the physical discrete state, which is used for calculating T^r_{dis}, and $|\psi(E_r)\rangle$ is the corresponding continuum state, which is used for calculating T^r_{con}. The interaction strength V_r is also related to the width Γ_r by

$$V_r=e^{i\phi_r}\sqrt{\frac{\Gamma_r}{2\pi}}, \tag{6}$$

where ϕ_r is the phase of the ratio $[(T^r_{con})^{\mu_i,\mu_b}_{\mu_0,\mu_a}(\mathbf{k}_0,\mathbf{k}_a,\mathbf{k}_b)/(T^r_{dis})^{\mu_i,\mu_b}_{\mu_0,\mu_a}(\mathbf{k}_0,\mathbf{k}_a,\mathbf{k}_b)]$ and has an implicit spin dependence.

Substituting $C(E_b)$ into Eq. (2) we obtain

$$(T^r_{res})^{\mu_i,\mu_b}_{\mu_0,\mu_a}(\mathbf{k}_0,\mathbf{k}_a,\mathbf{k}_b)=\frac{(T^r_{dis})^{\mu_i,\mu_b}_{\mu_0,\mu_a}(\mathbf{k}_0,\mathbf{k}_a,\mathbf{k}_b)-i\pi V_r^*(T^r_{con})^{\mu_i,\mu_b}_{\mu_0,\mu_a}(\mathbf{k}_0,\mathbf{k}_a,\mathbf{k}_b)}{(\epsilon_r+i)\pi V_r^*}. \tag{7}$$

Balashov *et al.* [6,7] showed that the angular distribution with respect to the ejected electron can be factored out of the T-matrix elements for each resonance. By setting

$$(T^r_{dis})^{\mu_i,\mu_b}_{\mu_0,\mu_a}(\mathbf{k}_0,\mathbf{k}_a,\mathbf{k}_b)=(G^r)^{\mu_i,\mu_b}_{\mu_0,\mu_a}(\mathbf{k}_0,\hat{\mathbf{k}}_a,\hat{\mathbf{k}}_b)\tau^r_{\mu_0,\mu_a}(\mathbf{k}_0,\mathbf{k}_a) \tag{8}$$

and

$$(T^r_{con})^{\mu_i,\mu_b}_{\mu_0,\mu_a}(\mathbf{k}_0,\mathbf{k}_a,\mathbf{k}_b)=(G^r)^{\mu_i,\mu_b}_{\mu_0,\mu_a}(\mathbf{k}_0,\hat{\mathbf{k}}_a,\hat{\mathbf{k}}_b)t^r_{\mu_0,\mu_a}(\mathbf{k}_0,\mathbf{k}_a) \tag{9}$$

we obtain

$$(T^r_{res})^{\mu_i,\mu_b}_{\mu_0,\mu_a}(\mathbf{k}_0,\mathbf{k}_a,\mathbf{k}_b)=\frac{(G^r)^{\mu_i,\mu_b}_{\mu_0,\mu_a}(\mathbf{k}_0,\hat{\mathbf{k}}_a,\hat{\mathbf{k}}_b)[\tau^r_{\mu_0,\mu_a}(\mathbf{k}_0,\mathbf{k}_a)-i\pi V_r^* t^r_{\mu_0,\mu_a}(\mathbf{k}_0,\mathbf{k}_a)]}{(\epsilon_r+i)\pi V_r^*}, \tag{10}$$

where $\tau^r_{\mu_0,\mu_a}(\mathbf{k}_0,\mathbf{k}_a)$ and $t^r_{\mu_0,\mu_a}(\mathbf{k}_0,\mathbf{k}_a)$ are the reduced excitation and ionization T matrices. It should be noted that the phase ϕ_r is also the phase of the $t^r_{\mu_0,\mu_a}(\mathbf{k}_0,\mathbf{k}_a)/\tau^r_{\mu_0,\mu_a}(\mathbf{k}_0,\mathbf{k}_a)$ ratio. The angular-distribution factor $(G^r)^{\mu_i,\mu_b}_{\mu_0,\mu_a}(\mathbf{k}_0,\hat{\mathbf{k}}_a,\hat{\mathbf{k}}_b)$ will be given explicitly later. When Eq. (10) is square integrated over all ejected-electron angles and summed over the ejected electron spin, one obtains Fano's formula for photoionization. The physical significance is that $(G^r)^{\mu_i,\mu_b}_{\mu_0,\mu_a}(\mathbf{k}_0,\hat{\mathbf{k}}_a,\hat{\mathbf{k}}_b)$ contains the effect of the angular distribution of the ejected electron. If the resonances are assumed to be nonoverlapping the total resonance amplitude can be expressed as a sum of the individual resonances

$$(T^{sum}_{res})^{\mu_i,\mu_b}_{\mu_0,\mu_a}(\mathbf{k}_0,\mathbf{k}_a,\mathbf{k}_b)=\sum_r\,(T^r_{res})^{\mu_i,\mu_b}_{\mu_0,\mu_a}(\mathbf{k}_0,\mathbf{k}_a,\mathbf{k}_b). \tag{11}$$

This was the formula used by Madison *et al.* [22].

B. Overlapping resonances treatment

For overlapping multiple resonances, the T_{res} part must be expressed as a weighted sum of each resonance. Thus following the matrix equations of Davis and Feldkamp [5] we obtain

$$(T^{mix}_{res})^{\mu_i,\mu_b}_{\mu_0,\mu_a}(\mathbf{k}_0,\mathbf{k}_a,\mathbf{k}_b)=\frac{\sum_r A^*_r(E_b)[(T^r_{dis})^{\mu_i,\mu_b}_{\mu_0,\mu_a}(\mathbf{k}_0,\mathbf{k}_a,\mathbf{k}_b)-i\pi V^*_r(T^r_{con})^{\mu_i,\mu_b}_{\mu_0,\mu_a}(\mathbf{k}_0,\mathbf{k}_a,\mathbf{k}_b)]}{[\epsilon_{eff}+i]\pi V^*_{eff}}. \tag{12}$$

We have used the label ''mix'' to indicate that each resonance is weighted by a mixing coefficient $A_r(E_b)$. As shown by Balashov *et al.* [6,7] we can factor out the angular-distribution term to obtain

$$(T^{mix}_{res})^{\mu_i,\mu_b}_{\mu_0,\mu_a}(\mathbf{k}_0,\mathbf{k}_a,\mathbf{k}_b)=\frac{\sum_r (G^r)^{\mu_i,\mu_b}_{\mu_0,\mu_a}(\mathbf{k}_0,\hat{\mathbf{k}}_a,\hat{\mathbf{k}}_b)A^*_r(E_b)[\tau^r_{\mu_0,\mu_a}(\mathbf{k}_0,\mathbf{k}_a)-i\pi V^*_r t^r_{\mu_0,\mu_a}(\mathbf{k}_0,\mathbf{k}_a)]}{[\epsilon_{eff}+i]\pi V^*_{eff}}. \tag{13}$$

A derivation of this formula is given in the Appendix. The quantities $\tau^r_{\mu_0,\mu_a}(\mathbf{k}_0,\mathbf{k}_a)$, $t^r_{\mu_0,\mu_a}(\mathbf{k}_0,\mathbf{k}_a)$, and $G^{r\mu_i,\mu_b}_{\mu_0,\mu_a}(\mathbf{k}_0,\hat{\mathbf{k}}_a,\hat{\mathbf{k}}_b)$ are the same quantities as in the nonoverlapping resonance approach. The effective ϵ parameter is defined as

$$\epsilon_{eff}=\left(\sum_r\,1/\epsilon_r\right)^{-1}. \tag{14}$$

The effective interaction strength V_{eff} is defined as

$$V_{eff}=\sum_r\,A_r(E_b)V_r, \tag{15}$$

where the $A_r(E_b)$ are the mixing coefficients used for mixing the resonances. They are a function of the ejected-electron energy. Both Fano and Davis and Feldkamp give $A_r(E_b)$ in the form

$$A_r(E_b)=\frac{V^*_r/(E_b-E_r)}{\left[\sum_s\,|V_s/(E_b-E_s)|^2\right]^{1/2}},\quad r=1,2,3\ldots. \tag{16}$$

As E_b approaches a particular resonance, the mixing coefficients of the other resonances will approach zero. Thus $A_r(E_{r'})=0$ for $r\neq r'$. In the form of Eq. (16), the mixing coefficients are not continuous at a resonance due to the fact that in the limit as the energy goes through a resonance we get

$$\lim_{E_b\to E^+_{r'}}\,A_r(E_b)e^{i\phi_r}=+\,\delta_{rr'}, \tag{17}$$

$$\lim_{E_b\to E^-_{r'}}\,A_r(E_b)e^{i\phi_r}=-\,\delta_{rr'}, \tag{18}$$

where the $+$ or $-$ on $E_{r'}$ indicates whether E_b is approaching $E_{r'}$ from above or below $E_{r'}$. Thus as the ejected electron energy E_b passes through a particular resonance with energy E_r from above to below E_r; the mixing coefficient of that resonance A_r will change from $+1$ to -1. It is explained in the appendix that by multiplying each of the mixing coefficients by the signum function, we can obtain continuity and still satisfy the matrix equation of Davis and Feldkamp [5] [Eq. (35) of their paper]. Thus we make the following replacement:

$$A_r(E_b)\to A_r(E_b)\Pi_s\,\mathrm{sgn}(E_s-E_b), \tag{19}$$

where $\mathrm{sgn}(E_s-E_b)$ is the sign of (E_s-E_b), which is either $+1$ or -1. This multiplication is not necessary theoretically;

TABLE I. LS coefficients ($\beta^r_{L,S}$) of the cadmium $4d^9 5s^2 5p$ autoionizing levels, their energies, and widths.

Resonance	^1P	^3P	^3D	Energy (eV)	Γ (eV)
1	−0.336961	−0.910489	0.239723	3.07	0.041
2	0.940191	−0.338915	0.34328	3.81	0.140
3	0.04999	0.236952	0.970234	3.94	0.003

however it makes the theory easier to understand and easier to compute numerically. With this replacement we now have

$$\lim_{E_b \to E_{r'}^-} A_r(E_b) e^{i\phi_r} = \lim_{E_b \to E_{r'}^+} A_r(E_b) e^{i\phi_r} = (-1)^r \delta_{rr'} . \tag{20}$$

It is also possible and convenient to multiply each mixing coefficient with the same constant phase. In this way one of the mixing coefficients can be made to be purely real.

In the experiments of Martin *et al.* [21] the triple differential cross section is obtained as a function of the energy of the slower electron. Therefore to compare with the experiments we need to calculate the triple differential cross section for the $(e,2e)$ process for cadmium where the energy of the incident electron is constant. There are three $J=1$ autoionizing resonances in our energy region of interest. The following sections shows how each term in Eq. (13) is calculated.

III. RESONANCE PART OF THE *T* MATRIX

In order to obtain the resonance part of the T matrix we need to describe the autoionizing states. For cadmium, there are several closely spaced autoionizing levels lying within 5 eV above the ionization potential (8.99 eV). The ground state of cadmium has a $4d^{10}5s^2$ configuration, the residual ion has a $4d^{10}5s$ configuration, and the autoionizing levels result primarily from the $4d^9 5s^2 5p$ configuration, which gives rise to several possible J states. Martin *et al.* [19] list 12 states lying between 3.07 eV and 5.07 eV above the ionization threshold. There are three autoionizing states with $J=1$. The autoionizing energies E_r and widths Γ_r are listed in Table I. There are three LS-coupled states in the $4d^9 5s^2 5p$ configuration that can contribute to a $J=1$ state. They are the $^1P_1$, $^3P_1$, and $^3D_1$ terms. The standard notation $^{2S+1}L_j$ is used here. The cadmium excited-state wave functions for $4d^9 5s^2 5p\ ^1P_1, ^3P_1, ^3D_1$ were constructed in the "frozen-core" approximation using the usual LS-term-dependent Hartree-Fock procedures. One obtains three $J=1$ states by taking different linear combinations of the three LS-coupled states. Thus the intermediate state composed of a scattered projectile state $(\mathbf{k}_a, \mu_a)$, which represents the final scattered state with the cadmium atom in a specific autoionizing resonance state r of energy E_r and J, M_J, is written as

$$\begin{aligned} |E_r, J, M_J, \mathbf{k}_a, \mu_a\rangle = {} & \beta^r_{1,0} |^1P_1, M_J, \mathbf{k}_a, \mu_a\rangle \\ & + \beta^r_{1,1} |^3P_1, M_J, \mathbf{k}_a, \mu_a\rangle \\ & + \beta^r_{2,1} |^3D_1, M_J, \mathbf{k}_a, \mu_a\rangle \end{aligned} \tag{21}$$

or more concisely as

$$|E_r, J, M_J, \mathbf{k}_a, \mu_a\rangle = \sum_{L,S} \beta^r_{L,S} |L, S, J, M_J, \mathbf{k}_a, \mu_a\rangle \tag{22}$$

Wilson [23] has calculated the coefficients for each of the three states using Hartree-Fock wave functions. However his results for the energies do not match exactly with the experimental resonance energies. Instead we are using the experimental values for E_r and Γ_r, which were obtained by Martin *et al.* [20,21] from the data. The β weighting coefficients are also taken from Martin [24]. He determined the β coefficients by adjusting Wilson's [23] results such that the three $J=1$ wave functions were orthogonal and yielded the experimental energies. These weighting coefficients that we have labeled as $\beta^r_{L,S}$ for the three $J=1$ states of interest are given in Table I .

The physical state that will autoionize is a result of excitation by an incident electron to all possible M_J substates. Consequently we define the physical state as a coherent sum over the possible M_J substates. This state will depend on the quantum numbers of both the incident and scattered projectiles. Thus we define

$$\begin{aligned} & |E_r, J, \mathbf{k}_0, \mu_0, \mathbf{k}_a, \mu_a\rangle \\ & \quad = \sum_{M_J} P^{r,J,M_J}_{\mu_0,\mu_a}(\mathbf{k}_0, \hat{\mathbf{k}}_a) |E_r, J, M_J, \mathbf{k}_a, \mu_a\rangle, \end{aligned} \tag{23}$$

where the partial fraction is defined as

$$P^{r,J,M_J}_{\mu_0,\mu_a}(\mathbf{k}_0, \hat{\mathbf{k}}_a) = \frac{\langle E_r, J, M_J, \mathbf{k}_a, \mu_a | T | \Phi_0, \mathbf{k}_0, \mu_0\rangle}{\left[\sum_{M_J} |\langle E_r, J, M_J, \mathbf{k}_a, \mu_a | T | \Phi_0, \mathbf{k}_0, \mu_0\rangle|^2 \right]^{1/2}} \tag{24}$$

and where Φ_0 is the ground-state atomic wave function. The partial fraction gives the complex fraction of the excitation to a particular M_J substate for a particular resonance r.

If the physical state in Eq. (23) is substituted into the T matrix we have

$$\begin{aligned} & \langle E_r, J, \mathbf{k}_0, \mu_0, \mathbf{k}_a, \mu_a | T | \Phi_0, \mathbf{k}_0, \mu_0\rangle \\ & \quad = \left[\sum_{M_J} |\langle E_r, J, M_J, \mathbf{k}_a, \mu_a | T | \Phi_0, \mathbf{k}_0, \mu_0\rangle|^2 \right]^{1/2} . \end{aligned} \tag{25}$$

This equation is equivalent to results given by Balashov *et al.* [6] and Madison *et al.* [22] who used a coherent sum on L, M_L states. The expression above can also be called as excitation amplitude. The semirelativistic approach of Madison and Shelton [25,26] and Madison *et al.* [27] is used for calculating this quantity. It is also related to the τ defined by Fano for a single resonance. Thus we define

$$\tau^r_{\mu_0,\mu_a}(\mathbf{k}_0,\mathbf{k}_a)=\langle E_r,J,\mathbf{k}_0,\mu_0,\mathbf{k}_a,\mu_a|T|\Phi_0,\mathbf{k}_0,\mu_0\rangle. \tag{26}$$

Following Balashov *et al.* [6] the reduced transition amplitude is combined with the angular-distribution part to obtain

$$(T^r_{dis})^{\mu_i,\mu_b}_{\mu_0,\mu_a}(\mathbf{k}_0,\mathbf{k}_a,\mathbf{k}_b) = (G^r)^{\mu_i,\mu_b}_{\mu_0,\mu_a}(\mathbf{k}_0,\hat{\mathbf{k}}_a,\hat{\mathbf{k}}_b)\,\tau^r_{\mu_0,\mu_a}(\mathbf{k}_0,\mathbf{k}_a). \tag{27}$$

The $(G^r)^{\mu_i,\mu_b}_{\mu_0,\mu_a}(\mathbf{k}_0,\hat{\mathbf{k}}_a,\hat{\mathbf{k}}_b)$ factor describes the angular distribution of the ejected slow electron and is given by

$$\begin{aligned}(G^r)^{\mu_i,\mu_b}_{\mu_0,\mu_a}(\mathbf{k}_0,\hat{\mathbf{k}}_a,\hat{\mathbf{k}}_b) &= \sum_{S,L,M_J} P^{r,J,M_J}_{\mu_0,\mu_a}(\mathbf{k}_0,\hat{\mathbf{k}}_a)\beta^r_{L,S} \\ &\times\langle L,M_L,\mu_i,\mu_b,\mathbf{k}_a,\mu_a|L,S,J,M_J,\mathbf{k}_a,\mu_a\rangle \\ &\times Y_{L,M_L}(\hat{\mathbf{k}}_b),\end{aligned} \tag{28}$$

where $\langle L,M_L,\mu_i,\mu_b,\mathbf{k}_a,\mu_a|$ is the uncoupled L,M_L state of the $4d^9 5s^2 5p$ configuration. In other words the partial-fraction $P^{r,J,M_J}_{\mu_0,\mu_a}(\mathbf{k}_0,\hat{\mathbf{k}}_a)$ weighting of the L,M_L states determines the coefficients for the Y_{L,M_L}'s. Explicitly, the general form is

$$\begin{aligned}(G^r)^{\mu_i,\mu_b}_{\mu_0,\mu_a}(\mathbf{k}_0,\hat{\mathbf{k}}_a,\hat{\mathbf{k}}_b) &= \sum_{S,L,M_J} P^{r,J,M_J}_{\mu_0,\mu_a}(\mathbf{k}_0,\hat{\mathbf{k}}_a)\beta^r_{L,S}C^{L,S,J}_{M_L,M_S,M_J} \\ &\times C^{1/2,1/2,S}_{\mu_i,\mu_b,M_S}Y_{L,M_L}(\hat{\mathbf{k}}_b).\end{aligned} \tag{29}$$

The contribution from the discrete states is much larger than the contribution from the continuum states. Thus only the partial fractions from the discrete states, $P^{r,J,M_J}_{\mu_0,\mu_a}(\mathbf{k}_0,\hat{\mathbf{k}}_a)$, are considered for the angular distribution. Here $C^{i,j,k}_{l,m,n}$ is a Clebsch-Gordon coefficient. The further decomposition of the L state in terms of the orbital angular momentum eigenstates of the ion l_{ion} and the ejected electron l_b is omitted because $l_{ion}=0$ in our case. Thus $L=l_b$ for this case. However it must be considered whenever the ion is not in an S state.

There will be a corresponding set of atomic states corresponding to the configuration $4d^{10}5s;\omega_r L$, where $\omega_r L$ corresponds to a continuum state with energy ω_r above the ionization energy such that $\omega_r=E_r$, with angular momentum L. We can write this state as a sum of substates of $|\Phi_{ion},\mu_i,\omega_r,L,M_L,\mu_b,\mathbf{k}_a,\mu_a\rangle$, where Φ_{ion} is the atomic state of the ion. The quantum numbers L,M_L,μ_b label the continuum wave function of the ejected electron. The physical state for the continuum [i.e., continuum equivalent to Eq. (22)] is obtained by coupling the ejected (slow) electron with the ion and forming a coherent sum on M_J. Thus we define

$$\begin{aligned}|\omega_r,J,\mathbf{k}_0,\mu_0,\mathbf{k}_a,\mu_a\rangle &= \sum_{L,M_L,\mu_i,\mu_b} \alpha^r_{\mu_0,\mu_a S,M_S}{}^{L,M_L}(\mathbf{k}_0,\hat{\mathbf{k}}_a)C^{1/2,1/2,S}_{\mu_i,\mu_b,M_S} \\ &\times|\Phi_{ion},\mu_i,\omega_r,L,M_L,\mu_b,\mathbf{k}_a,\mu_a\rangle.\end{aligned} \tag{30}$$

Since $\mu_i+\mu_b=M_S$ and $M_S+M_L=M_J$, summation on M_L implies a sum on M_J. Here we have defined

$$\alpha^r_{\mu_0,\mu_a S,M_S}{}^{L,M_L}(\mathbf{k}_0,\hat{\mathbf{k}}_a)=P^{r,J,M_J}_{\mu_0,\mu_a}(\mathbf{k}_0,\hat{\mathbf{k}}_a)C^{L,S,J}_{M_L,M_S,M_J}. \tag{31}$$

The same partial fractions are used for both the excitation and ionization amplitudes. For cadmium, L is the orbital angular momentum of the continuum electron l_b since the residual ion has zero angular momentum. It should be noted that Eq. (30) represents an atomic wave function with one of the orbitals being in a continuum state. The continuum part of the reduced resonance T matrix is given by

$$t^r_{\mu_0,\mu_a}(\mathbf{k}_0,\mathbf{k}_a)=\langle\omega_r,J,\mathbf{k}_0,\mu_0,\mathbf{k}_a,\mu_a|T|\Phi_0,\mathbf{k}_0,\mu_0\rangle \tag{32}$$

or

$$\begin{aligned}t^r_{\mu_0,\mu_a}(\mathbf{k}_0,\mathbf{k}_a) &= \sum_{L,M_L,\mu_i,\mu_b} \alpha^r_{\mu_0,\mu_a S,M_S}{}^{L,M_L}(\mathbf{k}_0,\hat{\mathbf{k}}_a)C^{1/2,1/2,S}_{\mu_i,\mu_b,M_S} \\ &\times\langle\Phi_{ion},\mu_i,\omega_r,L,M_L,\mu_b,\mathbf{k}_a,\mu_a|T|\Phi_0,\mathbf{k}_0,\mu_0\rangle.\end{aligned} \tag{33}$$

We write this as

$$t^r_{\mu_0,\mu_a}(\mathbf{k}_0,\mathbf{k}_a)=\sum_{L,M_L,\mu_i,\mu_b}(\alpha^r_{\mu_0,\mu_a})^{L,M_L}_{S,M_S}(\mathbf{k}_0,\hat{\mathbf{k}}_a) \times(I^r_{L,M_L})^{\mu_i,\mu_b}_{\mu_0,\mu_a}(\mathbf{k}_0,\mathbf{k}_a), \tag{34}$$

where $I^r_{L,M_L}{}^{\mu_i,\mu_b}_{\mu_0,\mu_a}(\mathbf{k}_0,\mathbf{k}_a)$ is the amplitude for the projectile electron to cause an excitation into a continuum state with energy ω_r, orbital angular momentum L, L projection M_L, spin projection μ_b, and at the same time be scattered into the direction defined by $\hat{\mathbf{k}}_a$ with spin projection μ_a. Its calculation is similar to the calculation of the direct amplitude $(T_{dir})^{\mu_0,\mu_a}_{\mu_i,\mu_b}(\mathbf{k}_a,\mathbf{k}_b)$ which is presented in the following section. The continuum equivalent of Eq. (26) is thus

$$(T^r_{con})^{\mu_i,\mu_b}_{\mu_0,\mu_a}(\mathbf{k}_0,\mathbf{k}_a,\mathbf{k}_b) = (G^r)^{\mu_i,\mu_b}_{\mu_0,\mu_a}(\mathbf{k}_0,\hat{\mathbf{k}}_a,\hat{\mathbf{k}}_b)t^r_{\mu_0,\mu_a}(\mathbf{k}_0,\mathbf{k}_a). \tag{35}$$

As pointed out before, T^r_{con} does not depend explicitly on the energy of the scattered electron because of energy conservation. Likewise I^r_{L,M_L} does not depend explicitly on the energy of the scattered electron.

IV. DIRECT KNOCKOUT AMPLITUDE

We use the standard first-order distorted-wave Born approximation (DWBA) for calculating direct knockout and ionization amplitudes such as $(T_{dir})^{\mu_i,\mu_b}_{\mu_0,\mu_a}(\mathbf{k}_a,\mathbf{k}_b)$ and $(I^r_{L,M_L})^{\mu_i,\mu_b}_{\mu_0,\mu_a}(\mathbf{k}_0,\mathbf{k}_a)$. For the direct knockout amplitude we follow the calculations of Madison *et al.* [22]. The details of the DWBA can be found in Refs. [28,29]. Since the electrons are identical particles, exchange also must be taken into account. From conservation of spin we know that $\mu_0=\mu_a+\mu_b+\mu_i$. As a result, the direct T matrix can be expressed as

$$(T_{dir})^{\mu_0,\mu_a}_{\mu_i,\mu_b}(\mathbf{k}_0,\mathbf{k}_a,\mathbf{k}_b)=(-1)^{1/2+\mu_0}[f\delta_{\mu_0,\mu_a}\delta_{\mu_i,-\mu_b}-g\delta_{\mu_0,\mu_b}\delta_{\mu_i,-\mu_a}], \tag{36}$$

where f is the direct scattering amplitude and g is the exchange amplitude. Equation (36) can be found in Ref. [22], as well as the following expressions for direct and exchange amplitudes:

$$f=\frac{4}{\sqrt{k_0^3k_ak_b}}\sum_{l_0l_al_bm_b}\frac{\hat{l}_0^2}{\hat{l}_a\hat{l}_b}i^{l_0-l_a-l_b}R^{k_0k_ak_b}_{l_0l_al_b}C^{l_0,l_a,l_b}_{0,m_b,m_b}\times C^{l_0,l_a,l_b}_{0,0,0}Y^*_{l_am_a}(\hat{\mathbf{k}}_a)Y_{l_bm_b}(\hat{\mathbf{k}}_b), \tag{37}$$

$$g=\frac{4}{\sqrt{k_0^3k_ak_b}}\sum_{l_0l_al_bm_b}\frac{\hat{l}_0^2}{\hat{l}_a\hat{l}_b}i^{l_0-l_a-l_b}R^{k_0k_bk_a}_{l_0l_al_b}C^{l_0,l_b,l_a}_{0,m_b,m_b}\times C^{l_0,l_b,l_a}_{0,0,0}Y^*_{l_am_a}(\hat{\mathbf{k}}_b)Y_{l_bm_b}(\hat{\mathbf{k}}_a), \tag{38}$$

where $\hat{l}=\sqrt{2l+1}$. The factor R, which contains all the radial integrals, is defined as

$$R^{k_0k_ak_b}_{l_0l_al_b}=\int_0^\infty\int_0^\infty\chi^a_{l_a}(\mathbf{k}_a,r_1)\chi^b_{l_b}(\mathbf{k}_b,r_2)\frac{r_<^{l_b}}{r_>^{l_b+1}}\times\psi_0(r_2)\chi^0_{l_0}(\mathbf{k}_0,r_1)dr_1dr_2. \tag{39}$$

Here χ is a distorted wave. The indices $0,a,b$ represent the incoming, faster, slower electrons, respectively, ψ_0 is the single-particle atomic wave function for the active electron and $r_<$ ($r_>$) is the usual lesser (greater) value for the two coordinates (r_1,r_2).

Finally the amplitude for exciting the continuum part of the autoionizing resonance, which is the $I^r_{L,M_L}{}^{\mu_i,\mu_b}_{\mu_0,\mu_a}(\mathbf{k}_0,\mathbf{k}_a)$ factor of Eq. (34), may be obtained as a subset of the amplitudes contained in Eqs. (37) and (38). For the present problem, the amplitude for exciting the atom into a state that has a continuum orbital with L is needed. This amplitude is obtained from Eqs. (37) and (38) by setting $l_b=L$, dropping the sum over m_b, and eliminating the spherical harmonic with $\hat{\mathbf{k}}_b$. So

$$(I^r_{L,M_L})^{\mu_i,\mu_b}_{\mu_0,\mu_a}(\mathbf{k}_0,\mathbf{k}_a)=(-1)^{1/2+\mu_0}[f^r_{L,M_L}\delta_{\mu_0,\mu_a}\delta_{\mu_i,-\mu_b}-g^r_{L,M_L}\delta_{\mu_0,\mu_b}\delta_{\mu_i,-\mu_a}], \tag{40}$$

$$f^r_{L,M_L}=\frac{4}{\sqrt{k_0^3k_ak_b}}\sum_{l_il_a}\frac{\hat{l}_0^2}{\hat{l}_a\hat{l}_b}i^{l_0-l_a-L}R^{k_0k_ak_b}_{l_0l_aL}\times C^{l_0,l_a,L}_{0,M_L,M_L}C^{l_0,l_a,L}_{0,0,0}Y^*_{l_am_a}(\hat{\mathbf{k}}_a), \tag{41}$$

where $\omega_r=k_b^2/2$ in atomic units,

$$g^r_{L,M_L}=\frac{4}{\sqrt{k_0^3k_ak_b}}\sum_{l_0l_a}\frac{\hat{l}_0^2}{\hat{l}_a\hat{L}}i^{l_0-l_a-L}R^{k_0k_bk_a}_{l_{0i}l_aL}\times C^{l_0,L,l_a}_{0,m_L,m_L}C^{l_0,L,l_a}_{0,0,0}Y_{L,M_L}(\hat{\mathbf{k}}_a). \tag{42}$$

V. TRIPLE DIFFERENTIAL CROSS SECTION

The triple differential cross section is defined as

$$\frac{d^3\sigma}{dE_bd\Omega_{k_a}d\Omega_{k_b}}=|T_{total}(\mathbf{k}_0,\mathbf{k}_a,\mathbf{k}_b)|^2 \tag{43}$$

In the preceding sections the T-matrix elements are defined in such a way that the normal flux factors are already included in the T-matrix elements. The formula for a single resonance r is

$$(T^r_{res})^{\mu_i,\mu_b}_{\mu_0,\mu_a}(\mathbf{k}_0,\mathbf{k}_a,\mathbf{k}_b)=\frac{(T^r_{dis})^{\mu_i,\mu_b}_{\mu_0,\mu_a}(\mathbf{k}_0,\mathbf{k}_a,\mathbf{k}_b)-i\pi V_r^*(T^r_{con})^{\mu_i,\mu_b}_{\mu_0,\mu_a}(\mathbf{k}_0,\mathbf{k}_a,\mathbf{k}_b)}{(\epsilon_r+i)\pi V_r^*}. \tag{44}$$

It is easy to see that for a single resonance all the asymmetry with respect to energy comes from the interference between the direct knockout amplitude and the resonance amplitude.

For many resonances using the nonoverlapping resonance approach of Eq. (11), the triple differential cross section is given by

$$|T_{total}(\mathbf{k}_0,\mathbf{k}_a,\mathbf{k}_b)|^2=|(T_{dir})^{\mu_0,\mu_a}_{\mu_i,\mu_b}(\mathbf{k}_0,\mathbf{k}_a,\mathbf{k}_b)|^2 + |(T^{sum}_{res})^{\mu_i,\mu_b}_{\mu_0,\mu_a}(\mathbf{k}_0,\mathbf{k}_a,\mathbf{k}_b)|^2 + 2\,\mathrm{Re}[(T_{dir})^{\mu_0,\mu_a}_{\mu_i,\mu_b}(\mathbf{k}_0,\mathbf{k}_a,\mathbf{k}_b) \times (T^{*sum}_{res})^{\mu_i,\mu_b}_{\mu_0,\mu_a}(\mathbf{k}_0,\mathbf{k}_a,\mathbf{k}_b)]. \quad (45)$$

As can be seen from Eq. (45) there will be cross terms associated with $|(T^{sum}_{res})^{\mu_i,\mu_b}_{\mu_0,\mu_a}(\mathbf{k}_0,\mathbf{k}_a,\mathbf{k}_b)|^2$ in addition to the cross terms with the direct amplitude. The cross terms between each resonance arise from

$$|(T^{sum}_{res})^{\mu_i,\mu_b}_{\mu_0,\mu_a}(\mathbf{k}_0,\mathbf{k}_a,\mathbf{k}_b)|^2 = \sum_r |(T^{r}_{res})^{\mu_i,\mu_b}_{\mu_0,\mu_a}(\mathbf{k}_0,\mathbf{k}_a,\mathbf{k}_b)|^2 + \sum_r \sum_{r'\neq r} 2\,\mathrm{Re}[(T^{r}_{res})^{\mu_i,\mu_b}_{\mu_0,\mu_a}(\mathbf{k}_0,\mathbf{k}_a,\mathbf{k}_b) \times (T^{*r'}_{res})^{\mu_i,\mu_b}_{\mu_0,\mu_a}(\mathbf{k}_0,\mathbf{k}_a,\mathbf{k}_b)], \quad (46)$$

and when written explicitly the energy dependence of the cross terms are

$$\sum_r \sum_{r'\neq r} 2\,\mathrm{Re}[(T^{r}_{res})^{\mu_i,\mu_b}_{\mu_0,\mu_a}(\mathbf{k}_0,\mathbf{k}_a,\mathbf{k}_b) \times (T^{*r'}_{res})^{\mu_i,\mu_b}_{\mu_0,\mu_a}(\mathbf{k}_0,\mathbf{k}_a,\mathbf{k}_b)] = \sum_r \sum_{r'\neq r} 2\,\mathrm{Re}\left[\frac{T^{r,r'}_{constant}}{(\epsilon_r+i)(\epsilon_{r'}-i)(\pi^2 V^*_r V_{r'})}\right], \quad (47)$$

where

$$T^{r,r'}_{constant}=[(T^{r}_{dis})^{\mu_i,\mu_b}_{\mu_0,\mu_a}(\mathbf{k}_0,\mathbf{k}_a,\mathbf{k}_b) - i\pi V^*_r (T^{r}_{con})^{\mu_i,\mu_b}_{\mu_0,\mu_a}(\mathbf{k}_0,\mathbf{k}_a,\mathbf{k}_b)] \times [(T^{*r'}_{dis})^{\mu_i,\mu_b}_{\mu_0,\mu_a}(\mathbf{k}_0,\mathbf{k}_a,\mathbf{k}_b) + i\pi V_{r'} (T^{*r'}_{con})^{\mu_i,\mu_b}_{\mu_0,\mu_a}(\mathbf{k}_0,\mathbf{k}_a,\mathbf{k}_b)] \quad (48)$$

is a constant amplitude as it is not a function of the ejected-electron energy. At a particular resonance energy $E_b=E_r$, the ϵ_r parameter vanishes. The contribution at the particular resonance r from the cross terms becomes

$$\sum_{r'\neq r} 2\,\mathrm{Re}\frac{T^{r,r'}_{constant}}{i(\epsilon_{r'}-i)\pi^2 V^*_r V_{r'}}. \quad (49)$$

So the magnitude of the contribution from the other resonances r' to that particular resonance r are directly proportional to the magnitude of both resonances and inversely proportional to the parameter $\epsilon_{r'}=(E_b-E_{r'})/(\Gamma_{r'}/2)$, which is the ratio of the energy difference to the half-width. The contribution is also strongly related to the phases. In our case the second resonance has the largest amplitude and the largest width so it has a big effect on the first and the third resonance. However the first resonance is too far from the second and the third resonance in the sense that the energy difference between them is much larger than the width of the resonance itself. This makes the $(E_1-E_2)/(\Gamma_1/2)$ too small to make any significant contribution near the second and third resonances. Similarly the third resonance has a very small value for the T matrix ($T^3_{res}\ll T^2_{res}$) so it does not make a significant contribution either.

When we introduce the mixing coefficients for the overlapping-resonance treatment, the direct part $|(T_{dir})^{\mu_0,\mu_a}_{\mu_i,\mu_b}(\mathbf{k}_a,\mathbf{k}_b)|^2$ does not change. However there are significant changes in the cross terms. At the exact resonance energy $E_b=E_{r'}$, Eq. (12) reduces to

$$|(T^{mix}_{res})^{\mu_i,\mu_b}_{\mu_0,\mu_a}(\mathbf{k}_0,\mathbf{k}_a,\mathbf{k}_b)|^2=\left|\frac{(T^{r'}_{dis})^{\mu_i,\mu_b}_{\mu_0,\mu_a}(\mathbf{k}_0,\mathbf{k}_a,\mathbf{k}_b)-i\pi V^*_{r'}(T^{r'}_{con})^{\mu_i,\mu_b}_{\mu_0,\mu_a}(\mathbf{k}_0,\mathbf{k}_a,\mathbf{k}_b)]}{i\pi V^*_{r'}}\right|^2, \quad (50)$$

since

$$\lim_{E_b\to E_{r'}} \epsilon_{eff}=0, \quad (51)$$

$$\lim_{E_b\to E_{r'}} A^*_r(E_b)=(-1)^{r'}\delta_{rr'}e^{i\phi_{r'}}, \quad (52)$$

$$\lim_{E_b\to E_{r'}} V^*_{eff}=(-1)^{r'}e^{i\phi_{r'}}V^*_{r'}. \quad (53)$$

The Kronecker delta reduces the r sum to 1; namely, the r' term. There is exactly zero contribution for the ''mix'' terms at the other resonances. Consequently, the cross terms do not contribute. This results in a relative decrease of the amplitudes in our case. The second resonance is almost not affected because the widths and amplitude of the first and the third resonances are small. However there is a significant decrease of the first resonance amplitude for all the angles, which results in a better agreement with the experiment. There is also a sharp minimum and maximum near the third resonance, which will be discussed in the following section.

VI. RESULTS

Martin *et al.* [21] have performed several coincidence measurements of $(e,2e)$ for cadmium. The incident electron's energy was held constant at 150 eV. In the final state a fast electron was detected for scattering angles ranging between 2° and 15°. Slow (ejected) electrons were detected by two detectors separated by 180°. The ejected-electron energies ranged from 2.6 eV to 4.6 eV to scan the energy region corresponding to the $J=1$ autoionizing levels of cadmium. All the angles in this paper are defined counterclockwise from the incident-beam direction in the scattering plane so that the angular range is from 0° to 360°. This is different from the angle convention used by Martin *et al.* [21]. The detectors for the slower electron are located at θ_{slow} and $\theta_{slow}-180°$. For each fast-electron scattering angle, the slow-electron detector angle θ_{slow} is chosen in three possible ways. It is either the momentum-transfer direction θ_{MT}, or $\theta_{MT}-\theta_{P2}$, or $\theta_{MT}-\theta_{P3}$, where θ_{P2} and θ_{P3} are the magic angles where the second- and third-order Legendre polynomials vanish, respectively. The momentum-transfer direction depends on both the ejected-electron energy and the fast-electron scattering angle. The sum and the difference of the counts from the two detectors were measured for those angles by Martin *et al.* [21].

The TDCS was calculated using both the overlapping-resonances approach and the nonoverlapping-resonances approach for the measured angles. The results were then summed for θ_{slow} and $\theta_{slow}-180°$ in order to compare with the experimental measurement. In Fig. 1 the experimental and theoretical results are compared for the fast-electron scattering at an angle of 2° measured counterclockwise from the incident direction. The slow electron's energy ranges from 2.6 eV to 4.6 eV. For this case the momentum-transfer direction θ_{MT} varies from 320° to 325°. The data in Fig. 1 correspond to one of the slow-electron detectors set to $\theta_{MT}-\theta_{P2}$ where $\theta_{P2}=54.7°$. For the energy range of the detected slow electrons θ_{slow} varies between 265° to 270°. Martin *et al.* [21] set the two detectors at $\theta_{slow}=270°$ and $\theta_{slow}-180°=90°$ for the whole energy range. The solid curve in the top portion of Fig. 1 is the present overlapping-resonances-treatment result and the dashed curve is the previous nonoverlapping-resonances-treatment result of the problem by Madison *et al.* [22]. The open circles are the summed experimental results of Martin *et al.* [21]. The experiment is normalized at the second (largest) resonance energy $E_2=3.81$ eV to the present calculation. From the figure it can be seen that the present approach predicts the height of the first resonance better than Madison *et al.* [22] and there is some sharp structure near the third resonance whereas there was no sharp structure in the Madison *et al.* [22] calculations. The sharp structure near the third resonance is characteristic of this approach and appears in all of the results.

The experimental resolution was given by Martin *et al.* [21] as 0.04 eV. The width of the third resonance is quite narrow ($\Gamma_3=0.003$ eV). Therefore we decided to convolute our results with the experimental energy-resolution function in order to ascertain its affect on the third resonance since the experimental results do not indicate any sharp structure at the third resonance. The solid curve in the bottom portion of Fig. 1 presents our result in the top portion of Fig. 1 convoluted with the experimental energy-resolution function. Again, the fast-electron scattering angle is 2° and our result is the sum of the slow ejected electrons detected at 270° and 90°. As can be seen, the sharp structure we find at the third resonance is washed out because of the energy resolution. Thus the sharp structure near the third resonance would not be detected by Martin *et al.* [21].

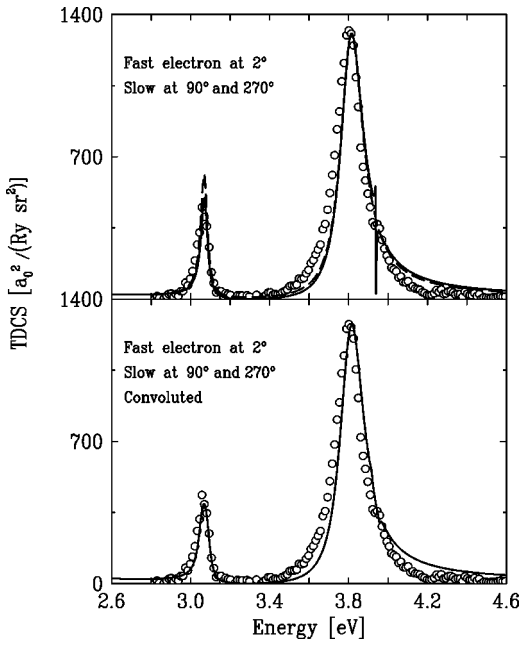

FIG. 1. Triple differential cross section (TDCS) for the fast electron scattered at 2° and the slow electron ejected at either 90° or 270°. The solid line in the top portion is for our present results based on the overlapping-resonances treatment of the problem. The dashed line is the previous results of Madison *et al.* [22] based on the nonoverlapping-resonances treatment of the problem. The open circles are the data labeled as $2P2$ sum by Martin *et al.* [21]. The bottom portion presents our results based on the overlapping-resonances treatment of the problem convoluted with the experimental energy resolution, which is 0.04 eV. The open circles are the data labeled as the $2P2$ sum by Martin *et al.* [21].

The characteristic line shape at the third resonance results from the interference between the direct and resonance parts of the T matrix as well as the phase difference between the mixing coefficients $A_2(E)$ and $A_3(E)$ near the third resonance. As is shown in the Appendix, the mixing coefficient $A_r(E)$ is proportional to V_r^*, which is defined as $e^{-i\phi_r}\sqrt{\Gamma_r/2\pi}$. In Fig. 2, $e^{i\phi_r}A_r(E)$ is plotted for the three autoionizing-resonance states as a function of energy for the energy region of interest. The function $e^{i\phi_r}A_r(E)$ equals $(-1)^r$ at the resonance corresponding to r and it equals zero at the other resonances. The $r=2$ resonance has the largest affect on the TDCS. This is because Γ_2 is three times larger than Γ_1 and over 46 times larger than Γ_3 (see Table I). It is seen from Fig. 2 that $e^{i\phi_2}A_2(E)$ changes sign as the energy crosses the third resonance. The rapid change in $e^{i\phi_2}A_2(E)$ from nearly $+1$ to almost -1 near the third resonance energy leads to constructive and destructive interference be-

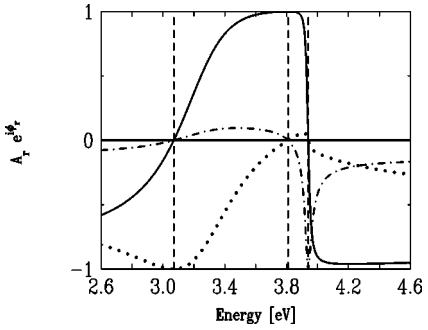

FIG. 2. Plot of $e^{i\phi_r}A_r(E)$ as a function of energy for the three resonances. Resonance energies E_r are marked as vertical dashed lines. The solid line is $e^{i\phi_2}A_2(E)$, which is the mixing coefficient for the second resonance. The dotted line is $e^{i\phi_1}A_1(E)$ and the dashed-dotted line is $e^{i\phi_3}A_3(E)$.

tween the direct and resonance parts of the T matrix, which is manifested in the characteristic line shape seen at the third resonance. For energies slightly less than the third resonance the interference is constructive and for energies slightly greater than the third resonance energy the interference is destructive. The slight rise in the TDCS as the ejected-electron energy approaches the third resonance is due to constructive interference. After the convolution of our results with the experimental resolution function there is still a small ''bump'' remaining, which originated from the constructive interference.

Figures 3–9 show our results for a sample of different scattering angles. Similar to Fig. 1, in the bottom part of Figs. 7 and 9 we show our present results convoluted with the experimental resolution function. Just as in Fig. 1 the sharp structure predicted at the third resonance is no longer apparent in Figs. 7 and 9 after convolution with the experimental resolution function. Overall the present results give a better fit to the ratio of peak heights, especially as the scattering angle becomes larger. For example, in Fig. 9 the scattering angle is 9° and the data were taken at angles corresponding to a zero of the third-order Legendre polynomial, $\theta_{P3}=39.2°$. Thus the detectors for the slower electron were set at $\theta_{slow}=\theta_{MT}-\theta_{P3}$ and $\theta_{MT}-\theta_{P3}-180°$. At this scattering angle θ_{MT} varies from 288.8° to 291.3° corresponding to a slow electron of energy 2.6 eV and 4.6 eV, respectively. Thus θ_{slow} varies from 249.6° to 252.1°. The average value of $\theta_{slow}\simeq 251°$. Therefore, the two electron detectors were set at 251° and 71° for the data in Fig. 9. It can be seen that the previous results of Madison *et al.* [22] yield a very poor fit to the ratio of the peak heights. Martin *et al.* [21] have also

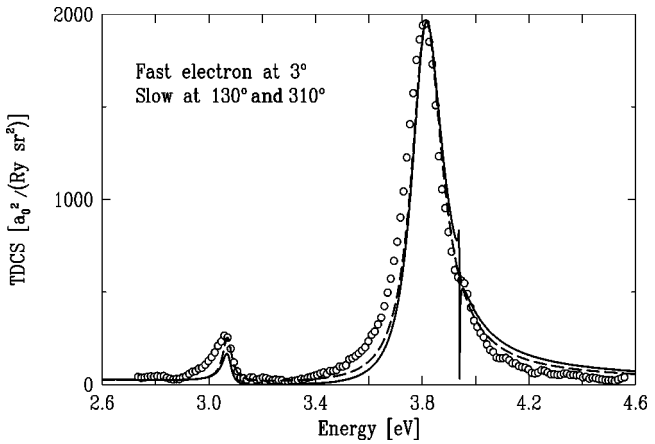

FIG. 3. Triple differential cross section (TDCS) for the fast electron scattered at 3° and the slow electron ejected at either 130° or 310°. The solid line is for our present results based on the overlapping-resonances treatment of the problem. The dashed line is for the previous results of Madison *et al.* [22] based on the nonoverlapping-resonances treatment of the problem. The open circles are the data labeled as 3MT sum by Martin *et al.* [21].

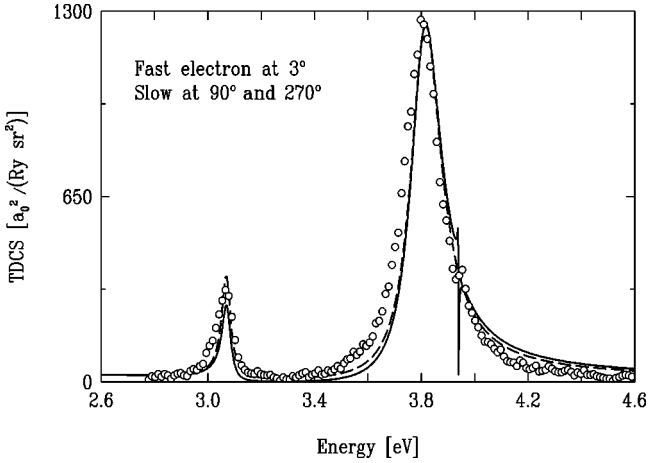

FIG. 4. Triple differential cross section (TDCS) for the fast electron scattered at 3° and the slow electron ejected at either 90° or 270°. The solid line is for our present results based on the overlapping-resonances treatment of the problem. The dashed line is for the previous results of Madison *et al.* [22] based on the nonoverlapping-resonances treatment of the problem. The open circles are the data labeled as $3P3$ sum by Martin *et al.* [21].

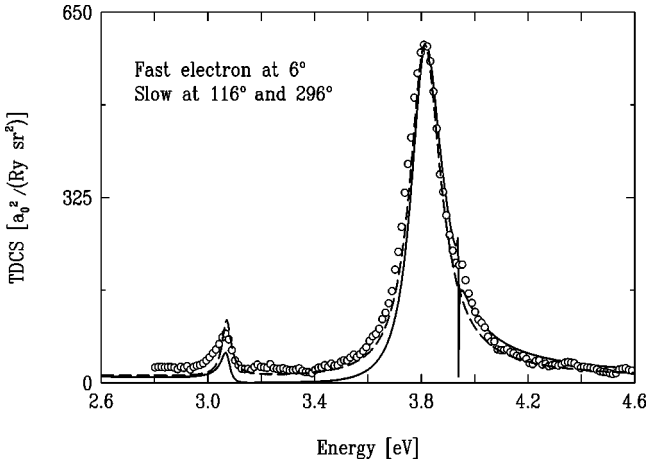

FIG. 5. Triple differential cross section (TDCS) for the fast electron scattered at 6° and the slow electron ejected at either 116° or 296°. The solid line is for our present results based on the overlapping-resonances treatment of the problem. The dashed line is for the previous results of Madison *et al.* [22] based on the nonoverlapping-resonances treatment of the problem. The open circles are the data labeled as 6MT sum by Martin *et al.* [21].

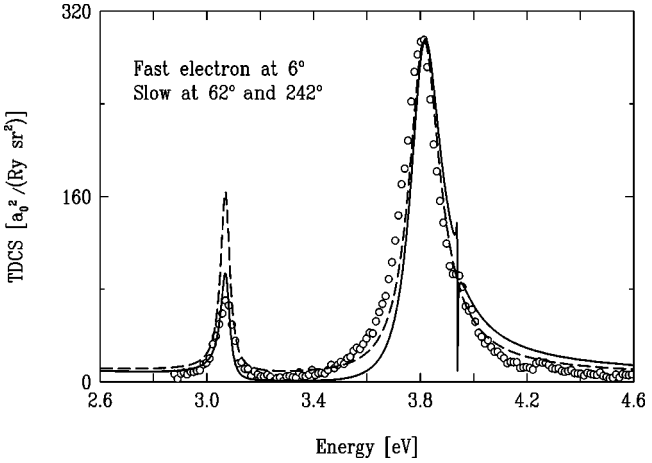

FIG. 6. Triple differential cross section (TDCS) for the fast electron scattered at 6° and the slow electron ejected at either 62° or 242°. The solid line is for our present results based on the overlapping-resonances treatment of the problem. The dashed line is for the previous results of Madison *et al.* [22] based on the nonoverlapping-resonances treatment of the problem. The open circles are the data labeled as $6P2$ sum by Martin *et al.* [21].

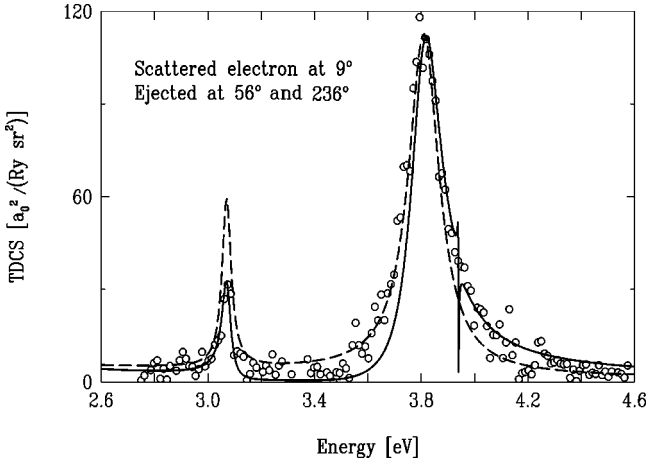

FIG. 8. Triple differential cross section (TDCS) for the fast electron scattered at 9° and the slow electron ejected at either 56° or 236°. The solid line is for our present results based on the overlapping-resonances treatment of the problem. The dashed line is for the previous results of Madison *et al.* [22] based on the nonoverlapping-resonances treatment of the problem. The open circles are the data labeled as $9P2$ sum by Martin *et al.* [21].

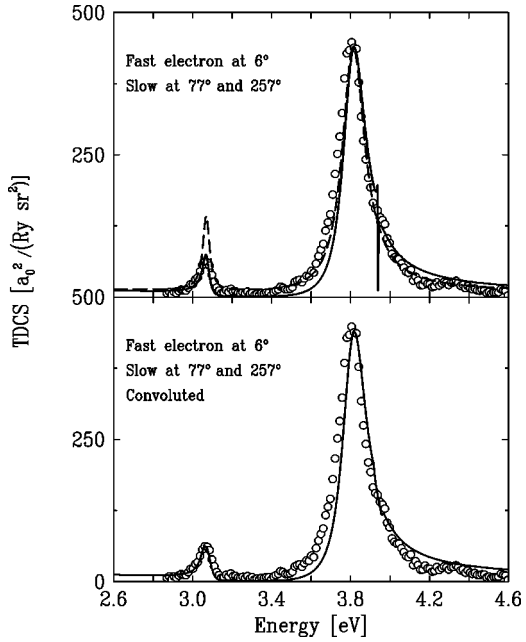

FIG. 7. Triple differential cross section (TDCS) for the fast electron scattered at 6° and the slow electron ejected at either 77° or 257°. The solid line in the top portion is for our present results based on the overlapping-resonances treatment of the problem. The dashed line is for the previous results of Madison *et al.* [22] based on the nonoverlapping-resonances treatment of the problem. The open circles are the data labeled as $6P3$ sum by Martin *et al.* [21]. The bottom portion presents our results based on the overlapping-resonances treatment of the problem convoluted with the experimental energy resolution, which is 0.04 eV. The open circles are the data labeled as the $6P3$ sum by Martin *et al.* [21].

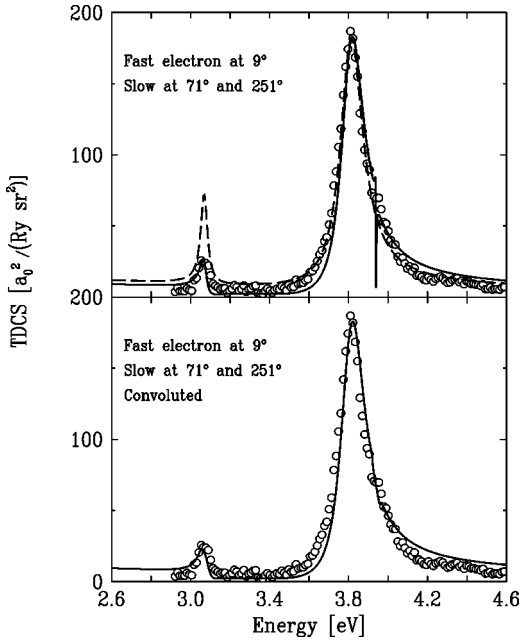

FIG. 9. Triple differential cross section (TDCS) for the fast electron scattered at 9° and the slow electron ejected at either 71° or 251°. The solid line in the top portion is for our present results based on the overlapping-resonances treatment of the problem. The dashed line is for the previous results of Madison *et al.* [22] based on the nonoverlapping-resonances treatment of the problem. The open circles are the data labeled as $9P3$ sum by Martin *et al.* [21]. The bottom portion presents our results based on the overlapping-resonances treatment of the problem convoluted with the experimental energy resolution, which is 0.04 eV. The open circles are the data labeled as the $9P3$ sum from Martin *et al.* [21].

calculated the TDCS. Their results also fail to give a good ratio of the peak heights for large angles. Neither the present results nor the previous results of Madison *et al.* [22] have quite the same shape as the experimental results. However it is interesting to note that the more elementary approach of Madison *et al.* [22] tends to predict the width and the shape of the second resonance better than the present approach.

VII. CONCLUSION

If the resonances are treated as overlapping resonances, we find that the mixing coefficients $A_r(E)$ are identically zero at all resonances except r. Therefore there is no interference between the resonances at an exact resonance energy [see Eqs. (17) and (18)]. Thus the TDCS value at the exact resonance energy is the same as the value obtained for a single resonance. However there is interference between the overlapping resonances for energies not equal to an exact resonance energy. For the problem considered here, the second resonance dominates the spectrum. The third resonance is very weak compared to the second resonance and this causes the second mixing term $e^{i\phi_2}A_2(E)$ to have a nearly step-function behavior at the third resonance. This behavior appears as constructive and destructive interference as the energy passes through the third resonance energy, which results in a very sharp characteristic line shape at the third resonance. The characteristic line shape results from the behavior of the mixing term $e^{i\phi_2}A_2(E)$ and the relative phases. Consequently the characteristic line shape is not necessarily a general feature of the many-overlapping-resonances treatment. For systems with different relative phases the effect would be different. However if we convolute our results with the experimental resolution function quoted by Martin *et al.* [21], the sharp structure at the third resonance dissappears. The only remnant after the convolution is a small ''bump'' near the third resonance.

Near the first resonance, the TDCS calculated using the overlapping-resonances treatment is always smaller than the TDCS calculated using the nonoverlapping-resonances treatment. This is due to the fact that the second resonance contributes near the first resonance in the nonoverlapping-resonances treatment, whereas in the overlapping-resonances treatment it does not contribute. Since the width of the second resonance Γ_2 is large, this contribution can be significant. As a result the present approach yields a much better peak-to-peak ratio between the first and the second resonances than was found in Madison *et al.* [22]

Neither our results nor the previous results of Madison *et al.* [22] yield a good fit to the shape of the second resonance. This shape is mainly determined by the phase of the second resonance $e^{i\phi_2}$. Different approaches for calculating continuum wave functions do not significantly change the magnitude of the $(I^r_{L,M_L})^{\mu_i,\mu_b}_{\mu_0,\mu_a}(\mathbf{k}_0,\mathbf{k}_a)$ amplitude. However different continuum waves would have different phases which determine the shape. Another explanation for the discrepancy in the shape is that a very basic approximation was used in Eq. (6) to obtain the phase of the interaction strength V_r. In that approximation we assumed that the discrete wave function is real and the phase should come only from the continuum wave function. However since the physical $J=1$ continuum state is constructed as a coherent sum, that sum as well as the spatial integral affects the phase. We conclude that a full theoretical calculation of the phase of the interaction strength $V_r=\langle\psi^r_J|V(1,2)|\Phi^r_J\rangle$ is needed to determine the shape better.

ACKNOWLEDGMENTS

The authors would like to acknowledge many helpful discussions with N. L. S. Martin. This project was supported by NSF.

APPENDIX

If we use the L,M_L,S,M_S,E quantum numbers to label the continuum states, there are two types of continuum states, namely, total-spin-singlet and -triplet states. Here S is constructed from the spin of the ion μ_i and the spin of the ejected electron μ_b. Since $l_{ion}=0$, L corresponds to the orbital angular momentum of the ejected electron l_b. However any L,M_L,S,M_S,E state can be written in terms of the coupled L,S,J,M_J,E states. These states are constructed from the L,M_L,S,M_S states via Clebsch-Gordan coefficients. Since we are dealing with autoionization of a specific $J=1$ state, the J states other than $J=1$ do not interfere with the discrete part of the wave function. Further, using a coherent sum on those indices, we can construct a single J state and express it with μ_0 and μ_a indices. This will correspond to the continuum part of the autoionizing state [Eq. (30)]. We assume that there is one type of continuum state as a function of energy for our autoionization problem. It is convenient to use the $K\geqslant N$ formalism of Davis and Feldkamp [5] with the number of continuum states equal to one ($k=1$) as mentioned. The fundamental equation is Eq. (35) of [5], namely,

$$[H_{nm}+F_{nm}-E\,\delta_{nm}]A_m+Z(E)V^*_{kn}V_{km}A_m=0 \quad \text{(A1)}$$

or

$$[H_{nm}+F_{nm}-E\,\delta_{nm}]A_m+Z(E)\Gamma_{nm}A_m=0, \quad \text{(A2)}$$

where

$$\Gamma_{nm}=V^*_{kn}V_{km} \quad \text{(A3)}$$

is the interaction matrix. The Einstein summation convention is used. The solution of this equation gives the mixing coefficients $A_r(E_b)$. The matrix F_{nm} is the energy-shift matrix. Since experimental values are used for the resonance energy and the LS coefficients of each resonance (Table I), we assume that the matrix $H_{nm}+F_{nm}$ is diagonalized and the effect of the energy shift is already included in the energy of the resonances. Thus we assume

$$H_{nm}+F_{nm}=E_n\delta_{nm}. \quad \text{(A4)}$$

In the main text V_r was defined in Eq. (6) as

$$V_r=e^{i\phi_r}\sqrt{\frac{\Gamma_r}{2\pi}}. \quad \text{(A5)}$$

For the V_r obtained from the Γ_r values in Table I, it is possible to separate the contribution from the singlet part and the triplet part as

$$\Gamma_n = \Gamma_{singlet,n} + \Gamma_{triplet,n}. \tag{A6}$$

This will give rise to a further separation of V_r to $V_{singlet,r}$ and $V_{triplet,r}$, which may be labeled as V_{1n} and V_{2n}. The many-discrete-states and many-continuum-states formalism of [5] should be used. However this separation does not affect the interaction matrix Γ_{nm}. Thus it does not change the mixing coefficients $A_r(E_b)$. Therefore we can use the $k=1$ formalism of [5]. For $k=1$ there is no sum on k in Eq. (A3). Thus we suppress the $k=1$ index and define

$$V_n = V_{1n} \tag{A7}$$

and the interaction matrix becomes

$$\Gamma_{nm} = V_{1n}^* V_{1m} = V_n^* V_m. \tag{A8}$$

With $k=1$, in the basis of the eigenstates of the Hamiltonian plus the energy shift, Eq. (A2) can be written as

$$\begin{pmatrix} E-E_1 & 0 & \cdots & 0 \\ 0 & E-E_2 & \cdots & 0 \\ \vdots & \vdots & \vdots & \vdots \\ 0 & 0 & \cdots & E-E_m \end{pmatrix} \begin{pmatrix} A_1 \\ A_2 \\ \vdots \\ A_m \end{pmatrix} = Z(E) \begin{pmatrix} \Gamma_{11} & \Gamma_{12} & \cdots & \Gamma_{1m} \\ \Gamma_{21} & \Gamma_{22} & \cdots & \Gamma_{2m} \\ \vdots & \vdots & \vdots & \vdots \\ \Gamma_{m1} & \Gamma_{m2} & \cdots & \Gamma_{mm} \end{pmatrix} \begin{pmatrix} A_1 \\ A_2 \\ \vdots \\ A_m \end{pmatrix}, \tag{A9}$$

where m labels a resonance. The elements of the normalized vector, which satisfies this equation, gives the mixing coefficients $A_r(E_b)$. Due to the symmetry of the matrix there is only one solution satisfying this matrix equation. If we take

$$\frac{1}{Z(E)} = \sum_{n=1}^{m} \frac{|V_n|^2}{(E-E_n)}, \tag{A10}$$

then we find that the solution vector given by

$$\vec{A}(E) = N(E) \begin{pmatrix} V_1^*/(E-E_1) \\ V_2^*/(E-E_2) \\ \vdots \\ V_m^*/(E-E_m) \end{pmatrix} \tag{A11}$$

satisfies the matrix equation. This corresponds to the $A_r(E)$ used in Eq. (16). It can also be found in Fano's paper. The factor $N(E)$ is a normalization factor. It is not necessary to normalize this vector because it appears in both the denominator and the numerator of the final formula for the T matrix. Furthermore, by multiplying this vector by the signum function, we can still keep the normalization and satisfy the matrix equation.

This definition of $Z(E)$ in Eq. (A10) corresponds to Eq. (60) in Fano's paper [1], namely,

$$\frac{\pi}{Z(E)} = -\tan(\Delta) = -\sum_n \tan(\Delta_n) = \sum_n \frac{\pi |V_n|^2}{E-E_n} = \sum_n \frac{1}{\epsilon_n}, \tag{A12}$$

$$Z(E)/\pi = \left(\sum_n 1/\epsilon_n \right)^{-1}, \tag{A13}$$

$$\epsilon_n = \frac{E-E_n}{\Gamma_n/2}. \tag{A14}$$

The transition rate is discussed in Sec. V of Fano's paper. The wave function that includes both discrete and continuum parts is expressed in Eq. (50) of Davis and Feldkamp's paper as

$$|\Psi(E)\rangle = C(E) \sum_n A_n(E) [|\Phi_n\rangle + Z(E) V_n |\psi(E_n)\rangle]. \tag{A15}$$

The index k and the energy dependence of the $|\Phi_n(E)\rangle$ and $|\psi(E)\rangle$ states used in their paper has been dropped. The coefficient A_n is the nth element of $\vec{A}(E)$ in Eq. (A11). We choose $C(E)$ such that

$$C(E)^{-1} = \pi \sum_n A_n(E) V_n [Z(E)/\pi - i], \tag{A16}$$

and substituting it into Eq. (A15) we have

$$|\Psi(E)\rangle = \frac{\sum_n A_n(E) |\Phi_n\rangle + Z(E) \sum_n A_n(E) V_n |\psi(E_n)\rangle}{[Z(E)/\pi - i] \sum_n \pi A_n(E) V_n}. \tag{A17}$$

Since A_n appears in both the numerator and the denominator, the normalization factor will cancel out and will not affect the calculated TDCS. That allows us to construct mixing coefficients that are continuous, with one of them real. The T-matrix element for the resonance process then becomes

$$\langle\Psi(E)|T|0\rangle=\frac{\sum_n A_n^*(E)\langle\Phi_n|T|0\rangle+Z(E)\sum_n A_n^*(E)V_n^*\langle\psi(E_n)|T|0\rangle}{\pi[Z(E)/\pi+i]\sum_n A_n^*(E)V_n^*}. \tag{A18}$$

When we add and subtract the term

$$\frac{[Z(E)/\pi+i]\sum_n A_n^*(E)V_n^*\langle\psi(E_n)|T|0\rangle}{[Z(E)/\pi+i]\sum_n A_n^*(E)V_n^*}, \tag{A19}$$

we obtain

$$\langle\Psi(E)|T|0\rangle=\frac{\sum_n A_n^*(E)V_n^*\langle\psi(E_n)|T|0\rangle}{\sum_n A_n^*(E)V_n^*}+\frac{\sum_n A_n^*(E)\langle\Phi_n|T|0\rangle-i\pi\sum_n A_n^*(E)V_n^*\langle\psi(E_n)|T|0\rangle}{\pi[Z(E)/\pi+i]\sum_n A_n^*(E)V_n^*}. \tag{A20}$$

The significance of this equation is that in Fano's formulation T_{dir} contains all the continuum states except the one that interferes with the discrete wave function. By taking out that part from the resonance T matrix and including it in the definition of T_{dir} we obtain an expression where T_{dir} contains all the continuum wave functions. Although in this form $\Sigma_n A_n^*(E)V_n^*$ does not cancel out to give exactly the appropriate continuum wave function, near resonances it will cancel out. Also at very large energies the deviation becomes significant. However, in our region of interest it is a very good approximation and is the proper way to express direct ionization. By defining

$$V_{eff}=\sum_n A_n(E_b)V_n, \tag{A21}$$

$$\epsilon_{eff}=\left(\sum_n 1/\epsilon_n\right)^{-1} \tag{A22}$$

and including the angular distribution function $(G^r)_{\mu_0,\mu_a}^{\mu_i,\mu_b}(\mathbf{k}_0,\hat{\mathbf{k}}_a,\hat{\mathbf{k}}_b)$ we obtain Eq. (13), namely,

$$(T_{res}^{mix})_{\mu_0,\mu_a}^{\mu_i,\mu_b}(\mathbf{k}_0,\mathbf{k}_a,\mathbf{k}_b)=\frac{\sum_r (G^r)_{\mu_0,\mu_a}^{\mu_i,\mu_b}(\mathbf{k}_0,\hat{\mathbf{k}}_a,\hat{\mathbf{k}}_b)A_r^*(E_b)[\tau_{\mu_0,\mu_a}^r(\mathbf{k}_0,\mathbf{k}_a)-i\pi V_r^* t_{\mu_0,\mu_a}^r(\mathbf{k}_0,\mathbf{k}_a)]}{[\epsilon_{eff}+i]\pi V_{eff}^*}. \tag{A23}$$

[1] U. Fano, Phys. Rev. **124**, 1866 (1961).
[2] U. Fano and J. W. Cooper, Phys. Rev. **137**, 1364 (1965).
[3] B. W. Shore, Rev. Mod. Phys. **39**, 439 (1967).
[4] D. G. McDonald and A. Crowe, J. Phys. B **25**, 4313 (1992).
[5] L. C. Davis and L. A. Feldkamp, Phys. Rev. B **15**, 2961 (1977).
[6] V. V. Balashov, S. S. Lipovetsky, and V. S. Senashenko, Zh. Eksp. Teor. Fiz. **63**, 1622 (1972) [Sov. Phys. JETP **36**, 858 (1973)].
[7] V. V. Balashov, S. E. Martin, and A. Crowe, J. Phys. B **29**, L337 (1996).
[8] A. S. Kheifets, J. Phys. B **26**, 2053 (1993).
[9] A. Pochat, R. J. Tweed, M. Doritch, and J. Peresse, J. Phys. B **15**, 2269 (1982).
[10] D. G. McDonald and A. Crowe, J. Phys. B **25**, 2129 (1992).
[11] O. Samardzic, A. S. Kheifets, E. Weigold, B. Shang, and M. J. Brunger, J. Phys. B **28**, 725 (1995).
[12] O. Samardzic, L. Campbell, M. J. Brunger, A. S. Kheifets, and E. Weigold, J. Phys. B **30**, 4383 (1997).
[13] G. Stefani, L. Avaldi, A. Duguet, and A. Lahmam-Bennani, J. Phys. B **19**, 3787 (1986).
[14] Z. P. Zhong, S. L. Wu, R. F. Feng, B. X. Yang, Q. Ji, K. Z. Zou, and J. M. Li, Phys. Rev. A **55**, 3388 (1997).
[15] J. W. G. Thomason and B. Peart, J. Phys. B **31**, L201 (1998).
[16] H. G. Teng, J. Phys. B **33**, L553 (2000).
[17] M. Khouilid, S. Cherkani-Hassani, N. Adimi, S. Rachafi, and P. Defrance, J. Phys. B **34**, 3239 (2001).
[18] N. L. S. Martin, J. Phys. B **23**, 2223 (1990).
[19] N. L. S. Martin, D. B. Thompson, R. P. Bauman, and M. Wilson, Phys. Rev. A **50**, 3878 (1994).

[20] N. L. S. Martin, R. P. Bauman, D. B. Thompson, M. Wilson, and K. J. Ross, J. Phys. B **29**, 4457 (1996).
[21] N. L. S. Martin, R. P. Bauman, and M. Wilson, Phys. Rev. **59**, 2764 (1999).
[22] D. H. Madison, V. D. Kravtsov, J. B. Dent, and M. Wilson, Phys. Rev. A **56**, 1983 (1997).
[23] M. Wilson, J. Phys. B **1**, 736 (1968).
[24] N. L. S. Martin (private communication).
[25] D. H. Madison and W. N. Shelton, Phys. Rev. A **7**, 499 (1973).
[26] D. H. Madison and W. N. Shelton, Phys. Rev. A **7**, 514 (1973).
[27] D. H. Madison, K. Bartschat, and R. Srivastava, J. Phys. B **24**, 1839 (1991).
[28] D. H. Madison, R. V. Calhoun, and W. N. Shelton, Phys. Rev. A **16**, 552 (1977).
[29] D. H. Madison, V. D. Kravtsov, S. Jones, and R. P. McEachran, Phys. Rev. A **53**, 2399 (1996).